

Thermal Decomposition Kinetics of Kerosene-Based Rocket Propellants. 1. Comparison of RP-1 and RP-2

Jason A. Widegren and Thomas J. Bruno*

Thermophysical Properties Division, National Institute of Standards and Technology (NIST), 325 Broadway,
Boulder, Colorado 80305-3328

Received June 5, 2009. Revised Manuscript Received August 27, 2009

The decomposition kinetics of the kerosene-based rocket propellants RP-1 and RP-2 was studied. For RP-2, decomposition reactions were performed at 375, 400, 425, and 450 °C. For RP-1, decomposition reactions were only performed at 450 °C because we had previously studied decomposition at 375, 400, and 425 °C. All of the decomposition reactions were performed in stainless-steel ampule reactors. At each temperature, the extent of decomposition as a function of time was determined by analyzing the thermally stressed liquid phase by gas chromatography. These data were used to derive global pseudo-first-order rate constants that approximate the overall rate of decomposition for the fuel. For RP-2, the rate constants ranged from $1.33 \times 10^{-5} \text{ s}^{-1}$ at 375 °C to $5.47 \times 10^{-4} \text{ s}^{-1}$ at 450 °C. The rate constants for the decomposition of RP-1 are not significantly different in that temperature range. One use of these rate constants is for the design and planning of physical property measurements at high temperatures. On the basis of the amount of time required for 1% of the sample to decompose ($t_{0.01}$), we found that allowable instrument residence times ranged from 15 min at 375 °C to 0.3 min at 450 °C.

Introduction

A large-scale project involving the thermophysical properties of kerosene-based fuels is in progress at the National

Institute of Standards and Technology (NIST) as well as other facilities.^{1–23} This work is meant to enhance design and operational specifications for these fluids and facilitate new applications.⁵ The thermophysical properties that are being measured include equilibrium properties (such as the fluid

*To whom correspondence should be addressed. Telephone: (303) 497-5158. Fax: (303) 497-5927. E-mail: bruno@boulder.nist.gov.

(1) Bruno, T. J.; Huber, M. L.; Laesecke, A.; Lemmon, E. W.; Perkins, R. A. Thermochemical and thermophysical properties of JP-10, NISTIR 6640. National Institute of Standards and Technology, Boulder, CO, June 2006.

(2) Bruno, T. J.; Smith, B. L. Improvements in the measurement of distillation curves. 2. Application to aerospace/aviation fuels RP-1 and S-8. *Ind. Eng. Chem. Res.* **2006**, *45* (12), 4381–4388.

(3) Magee, J. W.; Bruno, T. J.; Friend, D. G.; Huber, M. L.; Laesecke, A.; Lemmon, E. W.; McLinden, M. O.; Perkins, R. A.; Baranski, J.; Widegren, J. A. Thermophysical properties measurements and models for rocket propellant RP-1: Phase I, NISTIR 6646. National Institute of Standards and Technology, Boulder, CO, Feb 2007.

(4) Smith, B. L.; Bruno, T. J. Improvements in the measurement of distillation curves. 4. Application to the aviation turbine fuel Jet-A. *Ind. Eng. Chem. Res.* **2007**, *46* (1), 310–320.

(5) Wang, T. S. Thermophysics characterization of kerosene combustion. *J. Thermophys. Heat Transfer* **2001**, *15* (2), 140–147.

(6) Bruno, T. J. The properties of S-8 and JP-10. Technical Report to the Wright Laboratory Aero Propulsion and Power Directorate. National Institute of Standards and Technology, Boulder, CO, Nov 2007.

(7) Widegren, J. A.; Bruno, T. J. Thermal decomposition kinetics of the aviation turbine fuel Jet A. *Ind. Eng. Chem. Res.* **2008**, *47* (13), 4342–4348.

(8) Huber, M. L.; Smith, B. L.; Ott, L. S.; Bruno, T. J. Surrogate mixture model for the thermophysical properties of synthetic aviation fuel S-8: Explicit application of the advanced distillation curve. *Energy Fuels* **2008**, *22*, 1104–1114.

(9) Smith, B. L.; Bruno, T. J. Composition-explicit distillation curves of aviation fuel JP-8 and a coal-based jet fuel. *Energy Fuels* **2007**, *21* (5), 2853–2862.

(10) Smith, B. L.; Bruno, T. J. Application of a composition-explicit distillation curve metrology to mixtures of Jet-A and S-8. *J. Propul. Power* **2008**, *24* (3), 618–623.

(11) Outcalt, S. L.; Laesecke, A.; Brumback, K. J., Thermophysical properties measurements of rocket propellants RP-1 and RP-2. *J. Propul. Power* **2008**, manuscript submitted.

(12) Lovestead, T. M.; Bruno, T. J. Application of the advanced distillation curve method to aviation fuel avgas 100LL. *Energy Fuels* **2009**, *23*, 2176–2183.

(13) Lovestead, T. M.; Bruno, T. J. A comparison of the hypersonic vehicle fuel JP-7 to the rocket propellants RP-1 and RP-2 with the advanced distillation curve method. *Energy Fuels* **2009**, *23*, 3637–3644.

(14) Ott, L. S.; Hadler, A.; Bruno, T. J. Variability of the rocket propellants RP-1, RP-2, and TS-5: Application of a composition- and enthalpy-explicit distillation curve method. *Ind. Eng. Chem. Res.* **2008**, *47* (23), 9225–9233.

(15) Huber, M. L.; Lemmon, E.; Bruno, T. J. Effect of RP-1 compositional variability on thermophysical properties. *Energy Fuels* **2009**, in press.

(16) Huber, M. L.; Smith, B. L.; Ott, L. S.; Bruno, T. J. Surrogate mixture model for the thermophysical properties of synthetic aviation fuel S-8: Explicit application of the advanced distillation curve. *Energy Fuels* **2008**, *22*, 1104–1114.

(17) Huber, M. L.; Lemmon, E. W.; Diky, V.; Smith, B. L.; Bruno, T. J. Chemically authentic surrogate mixture model for the thermophysical properties of a coal-derived liquid fuel. *Energy Fuels* **2008**, *22*, 3249–3257.

(18) Huber, M. L.; Lemmon, E.; Ott, L. S.; Bruno, T. J. Preliminary surrogate mixture models for rocket propellants RP-1 and RP-2. *Energy Fuels* **2009**, *23*, 3083–3088.

(19) Bruno, T. J.; Huber, M. L.; Laesecke, A.; Lemmon, E. W.; Perkins, R. A. Thermochemical and thermophysical properties of JP-10, NIST-IR 6640. National Institute of Standards and Technology, Boulder, CO, 2006.

(20) Bruno, T. J. Thermodynamic, transport and chemical properties of “reference” JP-8. Book of Abstracts, Army Research Office and Air Force Office of Scientific Research, 2006 Contractor’s Meeting in Chemical Propulsion, 2006; pp 15–18.

(21) Bruno, T. J.; Laesecke, A.; Outcalt, S. L.; Seelig, H.-D.; Smith, B. L. Properties of a 50/50 mixture of Jet-A + S-8, NIST-IR-6647. National Institute of Standards and Technology, Boulder, CO, 2007.

(22) Smith, B. L.; Bruno, T. J. Composition-explicit distillation curves of aviation fuel JP-8 and a coal based jet fuel. *Energy Fuels* **2007**, *21*, 2853–2862.

(23) Smith, B. L.; Bruno, T. J. Application of a composition-explicit distillation curve metrology to mixtures of Jet-A + synthetic Fischer–Tropsch S-8. *J. Propul. Power* **2008**, *24* (3), 619–623.

density, vapor pressure, volatility, and heat capacity) and transport properties (such as viscosity and thermal conductivity). Some of these property data for RP-1 and RP-2 have already been reported.^{2,3,11,14,24,25} In those previous reports, we have described in detail the chemical and physical characteristics of the fluids that we discuss in this paper. The reader is referred to these sources for further information. The ultimate goal of the thermophysical property measurements is the development of equations of state to describe the properties.^{1,3,6,15–18} Such models are critical to all phases of design.²⁶

Understanding the thermal stability of RP-1 and RP-2 is important for a variety of reasons.^{24,27–32} One important motivation for our work was to ensure the quality of thermophysical property data that were collected at higher temperatures. The formation of both light and heavy decomposition products is a concern because either can cause significant changes in the properties of the fluid. Additionally, the formation of solid deposits inside instruments can cause systematic errors that are difficult to detect. However, if one understands the kinetics of decomposition, it is possible to avoid such problems by setting residence time limits for high-temperature measurements.³ In addition to impacting data quality, the formation of decomposition products can cause damage to the instruments themselves. Solid deposits (which plug capillaries, coat sensors, change internal volumes, etc.) can be difficult to remove. The formation of light decomposition products can result in a catastrophic increase in pressure in a closed system. Again, the key to avoiding such problems is to understand the kinetics of decomposition.

When planning high-temperature property measurements, it is useful to know the Arrhenius parameters for decomposition, which can be used to predict decomposition rates at any

given temperature. The Arrhenius parameters are determined from a plot of the rate constants for decomposition as a function of the temperature.^{7,24,33–37} In the case of complex mixtures, such as RP-1 and RP-2, rate constants for decomposition (and the Arrhenius parameters determined from them) will necessarily be approximate because they describe a complex series of reactions.^{7,24} Nevertheless, we have found that such an approach still yields information that is useful for determining residence-time constraints on measurements conducted at high temperature.

Herein, we report determinations of the thermal decomposition kinetics of RP-1 and RP-2 using a method that we previously developed for the kerosene-based fuels and organic Rankine cycle fluids.^{7,24,33} With this method, the fuel is thermally stressed in stainless-steel ampule reactors and the extent of decomposition is determined by monitoring the emergent suite of light, liquid-phase decomposition products. These data are used to derive pseudo-first-order rate constants that approximate the overall decomposition rate of the fuel. Rate constants for decomposition were determined at temperatures from 375 to 450 °C and were used to estimate Arrhenius parameters for the prediction of rate constants at other temperatures.

Theory

The thermal decomposition of fuels like RP-1 and RP-2 is very complex. There are a large number of compounds in each fuel; each compound may decompose by more than one reaction pathway; the decomposition reactions may yield more than one product; and the initial decomposition products may further decompose to other products. Also, the decomposition rate of a single component can be significantly altered in a mixture compared to that of the pure component.³⁸ Because of this complexity, a component-by-component analysis of the decomposition kinetics is simply not practical. Therefore, simplifying assumptions are necessary to gain insight into the overall thermal stability of these fuels. We made two such assumptions. First, we treated the kinetics as if we were dealing with a simple first-order reaction. Second, we assumed that the emergent suite of light, liquid-phase decomposition products is representative of all of the decomposition products. In this way, we derived “global” pseudo-first-order rate constants for the decomposition of the bulk fluid.^{39,40}

We monitored the increase in the emergent product suite as a function of time, t , during the decomposition reactions. At each temperature, data were collected at four different reaction times, with 3–5 replicate decomposition reactions run at each reaction time. Pseudo-first-order rate constants, k' , for decomposition were obtained by fitting these data to a first-order rate law, eqs 1–3, where $[B]_t$ is the concentration of products at time t and $[B]_\infty$ is the

(24) Andersen, P. C.; Bruno, T. J. Thermal decomposition kinetics of RP-1 rocket propellant. *Ind. Eng. Chem. Res.* **2005**, *44* (6), 1670–1676.

(25) Bruno, T. J. The properties of RP-1 and RP-2. Technical Report to AFRL/PRSA (Edwards Air Force Base), National Institute of Standards and Technology, Boulder, CO, March 2008.

(26) Bruno, T. J.; Billingsley, M.; Bates, R. W. Findings and recommendations from the Joint NIST/AFRL Workshop on Rocket Propellants and Hypersonic Vehicle Fuels. National Institute of Standards and Technology, Boulder, CO, Nov 2008.

(27) Bates, R. W.; Edwards, T.; Meyer, M. L. Heat transfer and deposition behavior of hydrocarbon rocket fuels. In 41st Aerospace Sciences Meeting and Exhibit, Reno, NV, 2003.

(28) Brown, S. P.; Frederick, R. A. Laboratory-scale thermal stability experiments on RP-1 and RP-2. *J. Propul. Power* **2008**, *24* (2), 206–212.

(29) Edwards, T.; Zabarnick, S. Supercritical fuel deposition mechanisms. *Ind. Eng. Chem. Res.* **1993**, *32* (12), 3117–3122.

(30) Stiegemeier, B.; Meyer, M. L.; Taghavi, R. A., Thermal stability and heat transfer investigation of five hydrocarbon fuels: JP-7, JP-8, JP-8 + 100, JP-10, RP-1. In 38th AIAA/ASME/SAE/ASEE Joint Propulsion Conference and Exhibit, Indianapolis, IN, 2002.

(31) Wohlwend, K.; Maurice, L. Q.; Edwards, T.; Striebich, R. C.; Vangness, M.; Hill, A. S. Thermal stability of energetic hydrocarbon fuels for use in combined cycle engines. *J. Propul. Power* **2001**, *17* (6), 1258–1262.

(32) MacDonald, M. E.; Davidson, D. F.; Hanson, R. K. Decomposition rate measurements of RP-1, RP-2, *n*-dodecane, and RP-1 with fuel stabilizers. In 44th AIAA/ASME/SAE/ASEE Joint Propulsion Conference and Exhibit, Hartford, CT, 2008.

(33) Andersen, W. C.; Bruno, T. J. Rapid screening of fluids for chemical stability in organic Rankine cycle applications. *Ind. Eng. Chem. Res.* **2005**, *44* (15), 5560–5566.

(34) Bruno, T. J.; Hume, G. L. A high-temperature, high-pressure reaction-screening apparatus. *J. Res. Natl. Bur. Stand.* **1985**, *90* (3), 255–257.

(35) Bruno, T. J.; Straty, G. C. Thermophysical property measurement on chemically reacting systems—A case study. *J. Res. Natl. Bur. Stand.* **1986**, *91* (3), 135–138.

(36) Straty, G. C.; Ball, M. J.; Bruno, T. J. PVT of toluene at temperatures to 673 K. *J. Chem. Eng. Data* **1988**, *33* (2), 115–117.

(37) Straty, G. C.; Palavra, A. M. F.; Bruno, T. J. PVT properties of methanol at temperatures to 300 °C. *Int. J. Thermophys.* **1986**, *7* (5), 1077–1089.

(38) Yu, J.; Eser, S. Supercritical-phase thermal decomposition of binary mixtures of jet fuel model compounds. *Fuel* **2000**, *79* (7), 759–768.

(39) Fodor, G. E.; Naegeli, D. W.; Kohl, K. B. Peroxide formation in jet fuels. *Energy Fuels* **1988**, *2* (6), 729–734.

(40) Lorant, F.; Behar, F.; Vandenbroucke, M.; McKinney, D. E.; Tang, Y. C. Methane generation from methylated aromatics: Kinetic study and carbon isotope modeling. *Energy Fuels* **2000**, *14* (6), 1143–1155.

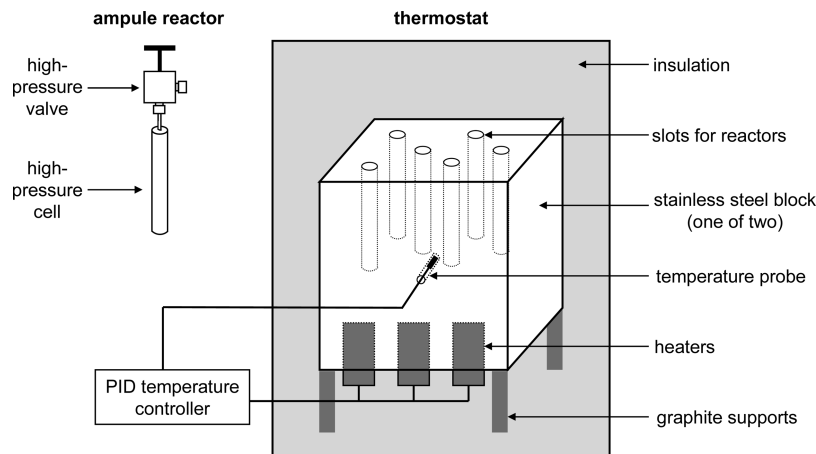


Figure 1. Apparatus used to thermally stress and decompose RP-1 and RP-2.

concentration of products at $t = \infty$



$$-d[A]/dt = d[B]/dt = k't \quad (2)$$

$$[B]_t = [B]_{\infty}(1 - \exp^{-k't}) \quad (3)$$

The half-life, $t_{0.5}$, at each temperature (i.e., the time required for one-half of the fuel to decompose) was then calculated from the rate constant using eq 4

$$t_{0.5} = 0.6931/k' \quad (4)$$

A related quantity is the time it takes for 1% of the fuel to decompose, $t_{0.01}$. For first-order reactions, $t_{0.01}$ is calculated from the rate constant using eq 5

$$t_{0.01} = 0.01005/k' \quad (5)$$

Finally, the rate constants for decomposition were used to evaluate the parameters of the Arrhenius equation

$$k' = A \exp(-E_a/RT) \quad (6)$$

Experimental Section

Chemicals. Reagent-grade acetone, toluene, and dodecane were used as solvents in this work. They were obtained from commercial sources and used as received. All had stated purities of no less than 99%, which is consistent with our own routine analyses of such solvents by gas chromatography. The RP-1 was obtained from the Fuels Branch of the Air Force Research Laboratory (AFRL, Wright Patterson Air Force Base) and was from a batch with the identification number POSF 4572. The RP-1 was pink because it contained the red dye azobenzene-4-azo-2-naphthol. The RP-2 was also obtained from the AFRL (Edwards Air Force Base). The RP-2 did not contain a dye; therefore, it was clear and colorless.

Apparatus. The apparatus used for the decomposition reactions is shown in Figure 1. Two thermostatted blocks of 304 stainless steel (AISI designation) were used to control the reaction temperature. Each block was supported in the center of an insulated box on carbon rods, which were chosen for their low thermal conductivity. A proportional-integral-derivative (PID) controller used feedback from a platinum resistance thermometer to maintain the temperature within 1 °C of the set value. As many as six stainless-steel ampule reactors could be placed into tight-fitting holes in each of the two thermostatted blocks. Each reactor consisted of a tubular cell with a

high-pressure valve. Each cell was made from a 5.6 cm length of ultra-high-pressure 316 L stainless-steel tubing (0.64 cm external diameter and 0.16 cm internal diameter) that was sealed on one end with a 316 L stainless-steel plug welded by a clean tungsten-inert-gas (TIG) process. The other end of each cell was connected to a valve with a 3.5 cm length of narrow-diameter 316 stainless-steel tubing (0.16 cm external diameter and 0.08 cm internal diameter) that was TIG-welded to the larger diameter tube. The valves were appropriate for high temperature in that the seats were stainless-steel and the packings were flexible-graphite. Each cell and valve was capable of withstanding a pressure of at least 100 MPa (15000 psi) at the temperatures used. The internal volume of each cell, including the short length of narrow connecting tubing but not including the relatively small noxious volume (i.e., swept dead volume) of the valve, was determined gravimetrically from the mass of toluene required to fill it. Each cell volume was determined several times, and the average value (approximately 0.11 mL) was used for subsequent calculations.

It is possible that the surface properties of the reactors change with age and use. This could potentially change the amount of surface-catalyzed decomposition and shift the observed rate constants for decomposition. Our experimental design accounts for such a possibility in the following way. At any one time, we have a set of 15 reactors that are used for decomposition studies. Individual reactors occasionally fail (by developing a leak, etc.) and are replaced by new reactors. Consequently, the set of reactors used for this decomposition study were of varying ages. Additionally, the different temperatures and reaction times were performed in a randomized order. Consequently, any effects of reactor aging should already be observable as scatter in the data (and, therefore, be included in the uncertainty estimates for the rate constants). Because scatter in the data is small, we conclude that surface aging in the reactors is not very important in this system. This conclusion also suggests that surface catalysis is not very important for these fluids.

Decomposition Reactions. The procedure used to fill the reactors was designed to achieve an initial target pressure of 34.5 MPa (5000 psi) for all of the decomposition reactions.²⁴ This is important because it mimics the high-pressure conditions during some physical property measurements and it helps ensure that differences in observed decomposition rates are only due to differences in temperature (and not to differences in pressure). With an equation of state for *n*-dodecane, a computer program⁴¹ calculated the mass of *n*-dodecane needed to achieve a pressure of 34.5 MPa at the given reaction temperature and cell

(41) Lemmon, E. W.; McLinden, M. O.; Huber, M. L. REFPROP, reference fluid thermodynamic and transport properties, version 7. National Institute of Standards and Technology, Gaithersburg, MD, 2002.

volume. We then assumed that the same mass of RP-1 or RP-2 would yield a pressure close to our target pressure. This is a reasonable assumption because, although the rocket propellants are complex mixtures, models derived from the properties of *n*-dodecane have been used successfully to approximate the physical properties of kerosene-based fuels.^{42,43} The calculated mass of RP-1 or RP-2 was added to the cell with a syringe equipped with a 26-gauge needle (sample masses were typically on the order of 0.06 g and varied depending upon the reaction temperature and cell volume). The valve was then affixed to the cell and closed. The cell was chilled to 77 K in liquid nitrogen, and subsequently, the head space was evacuated to 10 Pa through the valve to remove air from the cell. The valve was then reclosed, and the cell was warmed to room temperature. This single freeze–pump–thaw cycle removes the air from the vapor space in the cell without removing dissolved air from the fuel itself. This mimics the conditions under which the fuels are actually used (i.e., they contain dissolved air). The other advantage of doing only one freeze–pump–thaw cycle is that it limits the chances of removing more volatile components from the fuel. More rigorous degassing procedures, such as bubbling inert gas through the fuel, were avoided. Such procedures will cause a change in fuel composition by removing some of the more volatile components from the fuel. It is also worth mentioning that the autoxidation reactions caused by dissolved oxygen are thought to be relatively unimportant for hydrocarbon fuel decomposition above 250–300 °C.⁴⁴

The loaded reactors were then inserted into the thermostatted stainless-steel block, which was maintained at the desired reaction temperature. Fluid reflux inside the cells was minimized by putting the entire reactor inside the insulated box (although only the cell tubing was inserted into the thermostatted block). The reactors were maintained at the reaction temperature for a specified period ranging from 10 min to 24 h. To minimize the time required for temperature equilibration, only one reactor at a time was placed in the thermostatted block if the reaction time was less than 30 min. With this procedure, we estimate that the effective thermal equilibration (warm-up) time is approximately 2 min for a reaction temperature of 450 °C.⁴⁵ After decomposition, the reactors were removed from the thermostatted block and immediately cooled in room-temperature water. The thermally stressed fuel was then recovered and analyzed as described below.

After each run, the cells and valves were rinsed extensively with a mixture of acetone and toluene. The cells were also sonicated for 5 min (while filled with the acetone/toluene mixture) between rinsings to remove any solid deposits that may have formed on their walls. Cleaned cells and valves were heated to 150 °C for at least 1 h to remove residual solvent.

Blank experiments were occasionally performed to check the effectiveness of this protocol for cleaning the cells. For these blank experiments, a cell was loaded with fuel as described above but the cell was not heated above room temperature. After a day, the fuel in the cell was removed and analyzed by gas chromatography (GC) (as described in the following section). The success of the cleaning procedure was confirmed by the visual absence of color or solids in the unheated fuel and by the absence of decomposition products in the resulting gas chromatogram.

Analysis of Liquid-Phase Decomposition Products by GC. The production of light decomposition products caused the pressure

in the reactors to increase during the decomposition reactions. After decomposition, the reactors contained a pressurized mixture of vapor and liquid, even at room temperature. Liquid-phase decomposition products in the thermally stressed fuel were used to monitor the kinetics of decomposition. Therefore, a sampling procedure was designed to minimize the loss of the liquid sample when the reactors were opened. Specifically, a short length of stainless-steel tubing was connected to the valve outlet on the reactor. The end of this tubing was placed inside a chilled (7 °C) glass vial, and the valve was slowly opened. Often, some of the reacted fuel was expelled into the vial, especially for the more thermally stressed samples. The valve was then removed from the reactor, and any liquid remaining in the cell was transferred to the glass vial by use of a syringe with a 26-gauge needle. The vial was sealed with a silicone septum closure, and the mass of liquid sample was quickly determined (with an uncertainty of 0.0001 g). Then, the liquid sample was immediately diluted with a known amount of *n*-dodecane and refrigerated (at 7 °C) until the analysis was performed. The resulting *n*-dodecane solution was typically 5% reacted fuel (mass/mass). The purpose of this procedure was to prepare the samples for GC analysis and to minimize evaporative losses from the samples. One of the reasons for using *n*-dodecane is that it does not interfere with the GC analysis of early eluting decomposition products (see below).

Aliquots (3 μ L) from crimp-sealed vials of each sample were injected into a gas chromatograph equipped with an automatic sampler and a flame ionization detector (FID). Research-grade nitrogen was used as the carrier and makeup gas. The split/splitless injection inlet was maintained at 300 °C, and samples were separated on a 30 m capillary column coated with a 0.1 μ m film of (5% phenyl)-methylpolysiloxane.⁴⁶ A temperature program was used that consisted of an initial isothermal separation at 80 °C for 4 min, followed by a 20 °C/min gradient to 275 °C. This final temperature was held constant for 2 min. The FID was maintained at 275 °C.

RP-1 and RP-2 decomposition were observed from the total increase in the chromatographic peak areas of the emergent product suite. Chromatograms of unheated RP-1 and RP-2 exhibited only very small peaks with retention times of less than 3.2 min; however, following thermal stress, a suite of decomposition products was observed to elute earlier than 3.2 min. The total peak area of this suite of decomposition products was used for the kinetic analysis of decomposition. The peak area was corrected for dilution in *n*-dodecane by multiplying by the dilution factor. The peak area was also corrected for drifts in detector response by analyzing an aliquot of a stock solution (pentane and hexane in *n*-dodecane) along with each set of decomposition samples. Using the corrected peak areas as $[B]_t$, the kinetic data for each temperature were fit to eq 3 with a nonlinear least-squares program. Because of secondary decomposition (and long reaction times at the lower temperatures), it was not possible to determine experimentally a value for $[B]_{\infty}$. The recommended⁴⁷ procedure in such an instance is to treat $[B]_{\infty}$ as a floating variable (along with k') when fitting the kinetic data, which is what was done.

The simple use of peak area for the kinetic analysis is possible because of the types of compounds being analyzed and the use of a FID. For hydrocarbons, the relative sensitivity of the detector (on the basis of moles of carbon) varies by only a few percentages.⁴⁸ Consequently, calibrating the detector for each individual compound is not expected to significantly change the derived rate constants.

(42) Huber, M. L.; Laesecke, A.; Perkins, R. Transport properties of *n*-dodecane. *Energy Fuels* 2004, 18 (4), 968–975.

(43) Lemmon, E. W.; Huber, M. L. Thermodynamic properties of *n*-dodecane. *Energy Fuels* 2004, 18 (4), 960–967.

(44) Watkinson, A. P.; Wilson, D. I. Chemical reaction fouling: A review. *Exp. Therm. Fluid Sci.* 1997, 14 (4), 361–374.

(45) Widgren, J. A.; Bruno, T. J. Thermal decomposition kinetics of propylcyclohexane. *Ind. Eng. Chem. Res.* 2008, 48 (2), 654–659.

(46) Bruno, T. J.; Svoronos, P. D. N. *CRC Handbook of Basic Tables for Chemical Analysis*, 2nd ed.; CRC Press: Boca Raton, FL, 2003.

(47) Espenson, J. H. *Chemical Kinetics and Reaction Mechanisms*, 2nd ed.; McGraw-Hill: New York, 1995; p 25.

(48) McNair, H. M.; Bonelli, E. J. *Basic Gas Chromatography*; Varian: Palo Alto, CA, 1968.

Results and Discussion

Aliquots of RP-1 or RP-2 were thermally stressed in sealed stainless-steel ampule reactors with an initial pressure of 34.5 MPa (5000 psi). These conditions mimic the high-pressure conditions that existed during some of our physical property measurements. For RP-2, decomposition reactions were performed at 375, 400, 425, and 450 °C. For RP-1, decomposition reactions were only performed at 450 °C because we previously performed such measurements at 375, 400, and 425 °C.²⁴ This temperature range was chosen, in part, because it allowed for reaction times of a convenient length. At 375 °C, the reaction is relatively slow; therefore, reaction times ranged from 6 to 24 h. At 450 °C, the reaction is much faster; therefore, reaction times ranged from 10 to 40 min.

After each fuel was subjected to thermal stress, we made three types of qualitative observations related to thermal stability: (1) changes in color, (2) the development of coke deposits, and (3) the development of a pressurized vapor phase, which is caused by the formation of low-molecular-weight decomposition products. The unreacted RP-1 was pink (from the red dye in it). After 10 min at 450 °C, the pink color from the dye was entirely gone and the liquid was a pale yellow color. After 40 min at 450 °C, the liquid was yellowish brown in color with a small amount of black particulate. After thermally stressing RP-1 for 10 min at 450 °C, approximately half of the entire liquid sample was expelled under pressure when the reactor valve was opened. After 40 min at 450 °C, the entire liquid sample was expelled under pressure when the reactor valve was opened. The unreacted RP-2 was clear and colorless because it did not contain the red dye. After 10 min at 450 °C, it was still colorless. After 40 min at 450 °C, the liquid was yellowish brown in color with a very small amount of black particulate matter. After thermally stressing RP-2 for 10 min at 450 °C, approximately half of the entire liquid sample was expelled under pressure when the reactor valve was opened. After 40 min at 450 °C, the entire liquid sample was expelled under pressure when the reactor valve was opened. To summarize these qualitative observations of thermal stability, (1) RP-2 developed the yellowish brown color more slowly than RP-1, (2) RP-2 appeared to generate less coke than RP-1, but (3) both fuels generated similar amounts of vapor-phase cracking products.

Quantitative determinations of the thermal stability of RP-1 and RP-2 were based on the emergent suite of light, liquid-phase decomposition products. The thermally stressed liquid phase of every decomposition reaction was analyzed by a gas chromatograph equipped with a flame ionization detector (GC–FID). Figure 2 shows the early part of the chromatograms obtained for both thermally stressed and unstressed RP-1 and RP-2. The emergent product suite that was used for the kinetic analysis of the thermal stability of each fuel is circled in Figure 2. These peaks were chosen for two reasons: (1) they are relatively large, and (2) they occupy a part of the chromatogram that is devoid of any significant peaks for the unstressed fuels, which obviates the problems caused by peak overlap. Of course, many heavier decomposition products are formed simultaneously (as can be seen by the developing fine structure on the right-hand side of the chromatograms for the stressed fuels in Figure 2), but these are ignored in the current treatment. A study of the production of heavier decomposition products is an area for future research. It is interesting to note that the emergent product suites of RP-1 and RP-2 are

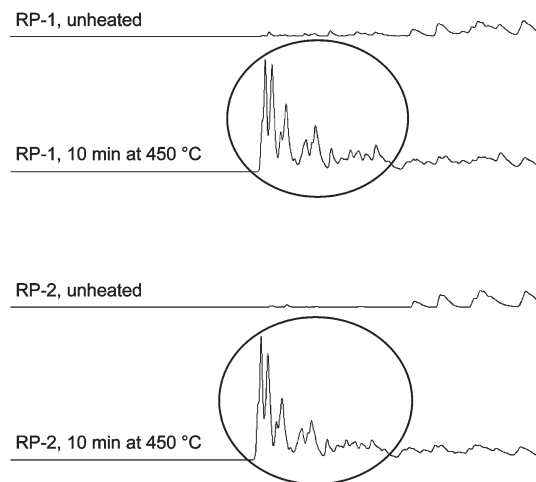


Figure 2. Initial part of the gas chromatograms for unheated RP-1 and RP-2 and for samples of each that had been thermally stressed at 450 °C for 10 min. In both cases, the emergent product suite that was used for the kinetic analysis is circled.

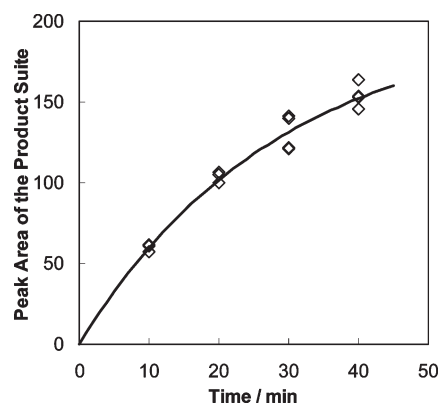


Figure 3. Plot of the corrected peak area of the emergent suite of light, liquid-phase decomposition products as a function of time. These data are for RP-1 being thermally stressed at 450 °C. Replicate decomposition reactions at each time point are shown as individual data points. The pseudo-first-order rate constant for thermal decomposition was determined from the nonlinear fit to the data (shown as a solid line).

remarkably similar, and even the relative abundances of products varied little in the temperature range studied.

Figure 3 shows the kinetic data for the decomposition of RP-1 at 450 °C. The value of k' was determined from the nonlinear fit to the data (the fit is shown as a solid line in Figure 3). For RP-1 at 450 °C, $k' = 5.84 \times 10^{-4} \text{ s}^{-1}$ with an uncertainty of $1.33 \times 10^{-4} \text{ s}^{-1}$. Values for $t_{0.5}$ and $t_{0.01}$ were calculated from k' using eqs 4 and 5. The decomposition rate constants for RP-1 at all four temperatures, along with values of $t_{0.5}$ and $t_{0.01}$, are presented in Table 1. The uncertainty for each value of k' in Table 1 is simply the standard error in the nonlinear fit. The values of $t_{0.01}$ show that an apparatus residence time of approximately 15 min may be acceptable for property measurements at 375 °C. On the other hand, at 450 °C, residence times longer than 0.3 min may be unacceptable.

Figure 4 shows the kinetic data for the decomposition of RP-2 at 450 °C. The value of k' was determined from the nonlinear fit to the data (the solid line in Figure 4). For RP-2 at 450 °C, $k' = 5.47 \times 10^{-4} \text{ s}^{-1}$ with a standard uncertainty of $0.80 \times 10^{-4} \text{ s}^{-1}$. Values for $t_{0.5}$ and $t_{0.01}$ were calculated from k' using eqs 4 and 5. The decomposition rate constants for RP-2

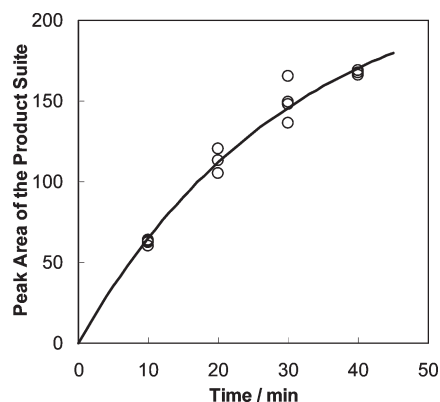


Figure 4. Plot of the corrected peak area of the emergent suite of light, liquid-phase decomposition products as a function of time. These data are for RP-2 being thermally stressed at 450 °C. Replicate decomposition reactions at each time point are shown as individual data points. The pseudo-first-order rate constant for thermal decomposition was determined from the nonlinear fit to the data (shown as a solid line).

Table 1. Kinetic Data for the Thermal Decomposition of RP-1

RP-1				
T (°C)	k' (s ⁻¹)	uncertainty in k' (s ⁻¹)	$t_{0.5}$ (h ⁻¹)	$t_{0.01}$ (min ⁻¹)
375	1.13×10^{-5a}	0.04×10^{-5}	17.0	14.8
400	1.19×10^{-4a}	0.33×10^{-4}	1.62	1.41
425	3.08×10^{-4a}	0.77×10^{-4}	0.63	0.54
450	5.84×10^{-4}	1.33×10^{-4}	0.33	0.29

^aThis rate constant was first reported earlier.²⁴

at all four temperatures, along with values of $t_{0.5}$ and $t_{0.01}$, are presented in Table 2. Again, the uncertainty for each value of k' in Table 2 is simply the standard error in the nonlinear fit.

A comparison of the rate constants in Tables 1 and 2 shows that the thermal stabilities of RP-1 and RP-2 are very similar. At every temperature except 425 °C, the rate constants for RP-1 and RP-2 are the same within their combined uncertainties (at 425 °C the rate constants differ by a little more than their combined standard uncertainties). From this data, we conclude that the thermal stabilities of RP-1 and RP-2 are not significantly different in the temperature range of 375–450 °C, at least with respect to the formation of light, liquid-phase decomposition products. This conclusion is consistent with our qualitative observations of the pressure increase caused by the formation of light, vapor-phase decomposition products (see above).

Figure 5 shows an Arrhenius plot of the rate constants for RP-1 and RP-2. The solid line in Figure 5 is a linear regression to the data for RP-2, which yields Arrhenius parameters of $A = 5.21 \times 10^9 \text{ s}^{-1}$ and $E_a = 180 \text{ kJ mol}^{-1}$. The uncertainty in E_a , calculated from the standard error in the slope of the regression, is 30 kJ mol⁻¹. Similarly, a linear regression to the data for RP-1 yields Arrhenius parameters of $A = 2.77 \times 10^{11} \text{ s}^{-1}$ and $E_a = 201 \text{ kJ mol}^{-1}$. The standard uncertainty in E_a , calculated from the standard error in the slope of the regression, is 39 kJ mol⁻¹. The relatively large uncertainties in the values of E_a are a reflection of the fact that the Arrhenius plots for RP-1 and RP-2 are not highly linear in the temperature range of these experiments. For both RP-1 and RP-2, the

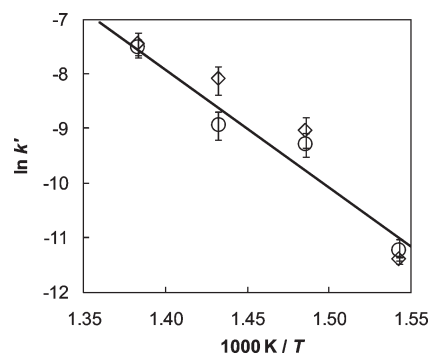


Figure 5. Arrhenius plot of the pseudo-first-order rate constants for the formation of light decomposition products. This figure demonstrates that RP-1 (◇) and RP-2 (○) decompose at similar rates over this temperature range. The error bars show the standard uncertainty. The solid line is a linear fit to the data for RP-2.

Table 2. Kinetic Data for the Thermal Decomposition of RP-2

RP-2				
T (°C)	k' (s ⁻¹)	uncertainty in k' (s ⁻¹)	$t_{0.5}$ (h ⁻¹)	$t_{0.01}$ (min ⁻¹)
375	1.33×10^{-5}	0.30×10^{-5}	14.5	12.6
400	9.28×10^{-5}	2.01×10^{-5}	2.07	1.80
425	1.33×10^{-4}	0.33×10^{-4}	1.45	1.26
450	5.47×10^{-4}	0.80×10^{-4}	0.35	0.31

activation energy for decomposition is lower than the values reported for pure C₁₀–C₁₄ *n*-alkanes; for example, for *n*-dodecane, E_a is 260 kJ mol⁻¹ (with a reported uncertainty of 8 kJ mol⁻¹).⁴⁹

A decomposition study by MacDonald et al. at Stanford provides an important point of comparison.³² In that work, RP-1 and RP-2 were decomposed at temperatures of 827–1027 °C (1100–1300 K) in an aerosol shock tube. In that temperature range, the decomposition rates for RP-1 and RP-2 were found to be quite similar.³² This important result combined with our work suggests that the decomposition rates (to light products) are similar over the entire temperature range of 375–1027 °C. It was also pointed out that a surprisingly linear Arrhenius plot can be made from the rate constants obtained at Stanford and NIST, despite the fact that the rate constants from the two studies span 8 orders of magnitude!³²

Conclusions

On the basis of the formation of light, liquid-phase decomposition products, we found that there is no significant difference between the thermal stability of RP-1 and RP-2 at temperatures of 375–450 °C and an initial pressure of 34.5 MPa. This knowledge is useful for planning physical and chemical property measurements at high temperatures and pressures. However, it is important to remember that the kinetics of decomposition may depend upon the identity of the wetted surfaces of the apparatus. Strictly speaking, these results are best applied when the wetted surface is constructed from 300 series stainless steels.

Acknowledgment. We gratefully acknowledge financial support from the Air Force Research Laboratory (AFRL) (MIPR F1SBAA8022G001). We thank Matthew Billingsley (AFRL, Edwards Air Force Base) and Ronald Bates (CPIAC) for useful discussions; we also thank Matthew Billingsley for supplying the RP-2. We thank Tim Edwards (AFRL, Wright Patterson Air Force Base) for supplying the RP-1.

(49) Yu, J.; Eser, S. Kinetics of supercritical-phase thermal decomposition of C₁₀–C₁₄ normal alkanes and their mixtures. *Ind. Eng. Chem. Res.* 1997, 36 (3), 585–591.